RESEARCH PAPER

A Physiologically Based Pharmacokinetic Model for Clobazam and Stiripentol in Adults and Children

Kayode Ogungbenro • Leon Aarons • and the CRESim & Epi-CRESim Project Groups

ABSTRACT

Purpose To develop a physiologically based pharmacokinetic model in adults and children for clobazam, its active metabolite norclobazam and stiripentol and to account for significant clinical interaction that has been reported when clobazam and stiripentol are co-administered.

Methods A PBPK model with ten compartments was developed. An *in vitro-in vivo* extrapolation technique was used to scale clearance in children for clobazam and norclobazam and clearance parameters for stiripentol were obtained from fitting. Other drug and system parameters were obtained from the literature.

Results The tissue/blood partition coefficients adequately predict observed volume of distribution for clobazam and stiripentol. In a clinical study in children where clobazam was administered alone and co-administered with stiripentol, the predicted and observed minimum concentration at steady state (mean and 95% confidence interval) during clobazam monotherapy were 0.19 (0.05–0.49 mg/L) and 0.20 (0.17–0.23 mg/L), respectively, and predicted and observed norclobazam concentrations were 0.49 (0.16–1.38 mg/L) and 0.95 (0.91–0.99 mg/L), respectively. From an interaction study with stiripentol the predicted stiripentol concentration was 10.12 (2.51–39.36 mg/L) and the observed concentration was 10.0 (8.3–11.7 mg/L); the predicted clobazam concentration was 0.29 (0.07–1.05 mg/L) and the observed concentration was 0.31 (0.24–0.38 mg/L); and the predicted norclobazam concentration was 2.30 (0.45–5.53 mg/L) and the observed concentration was 4.32 (3.77–4.87 mg/L).

Conclusions The PBPK model adequately described observed data and the extent of interaction between clobazam/norclobazam and stiripentol.

K. Ogungbenro (✉) • L. Aarons · CRESim & Epi-CRESim Project Groups
Centre for Applied Pharmacokinetic Research, Manchester Pharmacy
School, The University of Manchester
Oxford Road, Manchester M13 9PT, UK
e-mail: kayode.ogungbenro@manchester.ac.uk

INTRODUCTION

Severe myoclonic epilepsy in infants (SMEI) also known as Dravet syndrome (DS) is a rare form of epilepsy that affects at least one in 40,000 children up to the age of 7 years, it accounts for about 7% of severe forms of epilepsy in children under the age of 3 years [1, 2]. The seizures associated with DS are known to be some of the most resistant to conventional therapies. A number of studies have investigated existing and newer drugs including combinations of drugs for the treatment of DS. Drugs such as lamotrigine, vigabatrin and carbamazepine have been implicated in exacerbation of seizure [2–4] and treatments that include others such as clobazam (CLB), valproic acid (VPA), levetiracetam, zonisamide, topiramate and stiripentol (STI) have shown positive effect in the treatment of DS. The best results to date were obtained in a combination therapy involving CLB, STI and VPA in a randomised placebo controlled trial [5]. In this study, DS patients on CLB and VPA were randomised into STI or placebo arms in a double blind manner to investigate the effect of STI as add-on therapy. This combination proved effective in reducing the frequency of seizure in DS. Subsequently, both in the Europe and United States, STI was granted orphan drug status by the EMEA and FDA indicated for the treatment of DS [2, 3].

CLB is a 1,5-benzodiazepine, its pharmacokinetics (PK) has been extensively reviewed in the literature: it is rapidly absorbed following oral dosing; it reaches a peak within 2 h; and has a half-life ($t_{1/2}$) of between 10–50 h in healthy young subjects [6]. The route of administration of CLB is mainly oral. CLB's major metabolic pathway is dealkylation to N-desmethylclobazam also known as norclobazam (NCLB).

Both CLB and NCLB are pharmacologically active although NCLB has less pharmacological activity, its $t_{1/2}$ is longer, about four times that of CLB, and therefore has much higher plasma concentrations at steady state, suggesting it may contribute more to pharmacological activity following multiple dosing. Conversion of CLB to NCLB is by CYP3A4, CYP2C19 and CYP2B6 [7]. CLB is also metabolised to hydroxyclobalzam (OH-CLB) by CYP2C19 and CYP2C18 although this is a minor route of elimination of CLB [7]. Both NCLB and OH-CLB can be further metabolised into hydroxydesmethylclobazam (OH-NCLB). NCLB is metabolised predominantly by CYP2C19. CLB is widely distributed in the body and the apparent volume of distribution is around 1 L/kg [8]. Plasma protein binding of CLB and NCLB are 0.87 and 0.7 respectively [8].

STI is an antiepileptic drug that has shown remarkable results as add-on therapy with CLB and VPA [9]. Following oral administration, STI is rapidly and extensively absorbed from the gastro-intestinal tract, maximum concentration (C_{max}) is reached within 2 h of administration [4]. Although the absolute bioavailability of STI is not known, more than 70% of the administered dose can be accounted for in urine [4]. The most important route in the biotransformation of STI involves the opening of the methylenedioxy ring to generate catechol derivatives (50% of acute dose and 67% of chronic dose [10]). Glucuronidation is another important route, (22% of acute dose and 30% of chronic dose [10]). STI distributes extensively into body tissues and the apparent volume of distribution is 2.4 L/kg in healthy adult male volunteers [11] and 3.2 L/kg in children [4]. STI is highly bound to plasma protein, approximately 0.99 [12].

Although several metabolites have been reported following administration of STI in man, the enzymes and the mechanisms involved are still not well understood [10]. However, it has been shown both by *in vitro* and *in vivo* experiments that STI is a potent inhibitor of a wide range of CYP enzymes i.e. CYP1A2, CYP2C19, CYP3A4 and CYP2D6 at therapeutic concentrations [13, 14]. Consequently this leads to increased plasma concentration of other co-administered drugs with potential consequences for clinical outcomes. Clinically such interactions have been reported between STI and other anti-convulsant drugs such as carbamazepine, phenytoin and CLB [15]. In a placebo-controlled clinical trial where DS patients were randomised into CLB and VPA and CLB, VPA and STI arms, addition of STI to the CLB and VPA combination has been reported to produce modest increases in the plasma concentration of VPA and a marked increase in the plasma concentration of CLB and NCLB [5]. The effect of STI has been reported to have contributed to the efficacy reported for the combination and this may have also contributed to the side-effects.

This work forms part of the CRESim (Child Rare Euro-Simulation) project funded by ERA-NET PRIOMEDCHILD (http://www.priomedchild.eu/) and designed to investigate the use of modelling and simulation in the development of drugs for rare diseases. In this case the disease condition is DS and the drugs of choice are STI, CLB and VPA. The aims are to develop a physiologically based pharmacokinetic (PBPK) model for plasma and tissue concentration prediction for use in clinical trial simulation and to investigate using the PBPK model, changes in plasma concentration of CLB and NCLB with age and to predict changes in CLB/NCLB concentrations when CLB is co-administered with STI.

MATERIALS AND METHODS

PBPK Model Development and Assumptions

This work focused mainly on the development of a PBPK model for CLB and NCLB as well as STI. The model incorporated inhibition of CLB and NCLB metabolism by STI reported in the literature based on evidence from *in vitro* and *in vivo* experiments. The model was developed for adults and scaled to children using age-dependent changes in anatomical and physiological functions. Variability on system and drug-specific parameters were also introduced to simulate observed plasma concentrations.

The PBPK model developed for STI, CLB and NCLB is shown in Fig. 1. The model has ten compartments for gut lumen, enterocyte, gut tissue, systemic blood, kidney, liver, brain, spleen, muscle and rest of body. All tissues were modelled assuming a flow limited assumption, described by Eq. (1)

$$V_T \frac{dC_T}{dt} = Q_T\left(C_b - \frac{C_T}{K_{p,T}}\right) \tag{1}$$

where V_T, C_T, Q_T, and $K_{p,T}$ respresent the volume, concentration, blood flow, tissue/plasma concentration ratio of the different tissues and C_b is the systemic blood concentration. Oral administration is into the gut lumen from where it is absorbed by a first order process via the gut wall.

System Parameters

The model was developed for adults and scaled to children. System parameters were obtained for adults (18–20 years and 70 kg) from the literature for organ/tissue volumes, blood flows, cardiac output and other parameters. Also reference values were obtained for children at different age groups (0, 1, 5, 10, 15 years) from the literature to account for age-dependent changes in anatomical and physiological parameters such as organ/tissue volumes and blood flows [16]. Age-dependent changes in body size descriptors such as body
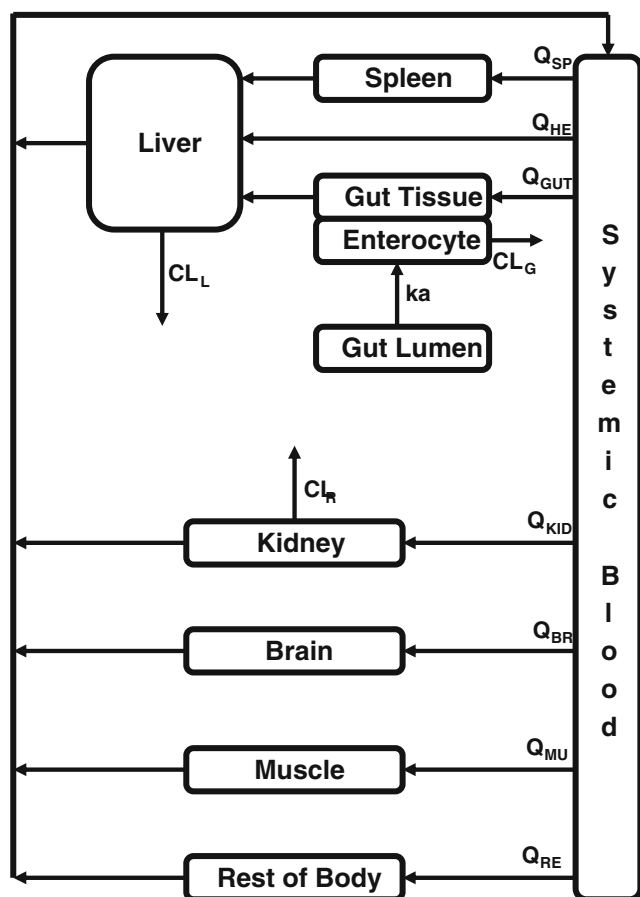
Fig. 1 Physiologically based pharmacokinetic model for clobazam/norclobazam (CLB/NCLB) and stiripentol (STI).

weight (BW) and height were also obtained from the literature, these were used to predict body surface area (BSA) using the Haycock and Dubois equations [17, 18]. Cardiac output in children was predicted using the equation developed by Johnson *et al.* [19]. For Monte Carlo simulation purposes, reference values for organ/tissue volumes and blood flows were expressed as functions of BW and cardiac output at the

reference age groups for children and adults. For ages in between the reference age groups, simple linear interpolation was used to simulate fractions of body weight and cardiac output for different tissues, these were converted to organ/tissue volumes and blood flows using simulated weight and cardiac output. Table I shows organ/tissue volumes and blood flows for adults and Table II shows other system parameters that have been used to scale metabolic parameters in the gut and the liver from *in vitro* systems.

Drug Specific Parameters

Tissue/blood concentration ratios (K_p) were predicted for CLB, NCLB and STI using the equations proposed by Rodgers and Rowland [20, 21]. K_ps for the rest of body compartment were obtained by lumping other tissues that have not been accounted for explicitly in the model, values for the K_ps for different tissues are shown in Table I. Other drug specific parameters used in the prediction of the kinetics of CLB, NCLB and STI are shown in Table III.

Clobazam/Norclobazam

The developed PBPK model for CLB and NCLB was based on the assumption that CLB is metabolised only to NCLB and NCLB is metabolised only to OH-NCLB in the gut and the liver. The conversion of CLB to NCLB in the gut is by CYP3A4 and CYP2C19 and the metabolic intrinsic clearance of CLB (also the formation clearance of NCLB) in the gut was given by Eq. 2 (for the linear range).

$$Clint, gut(CLB) = ESF_{CLB} \cdot \sum_i \frac{Vmax_i}{Km_i} \cdot ISEF_i \cdot Sca_i \quad (2)$$

where $i = CYP3A4$ and $CYP2C19$, $ISEF$ is the intersystem extrapolation factor, Sca is the total gut scaling factor which is related to the enzyme abundance in the gut, ESF is

Table I Organ Volumes (V), Blood Flows (Q) and Tissue/Blood Concentration Ratio (K_p) for Different Tissues/Organs and Drugs in Adults

Parameters	Organs/tissues								
	Systemic blood	Kidney	Liver	Gut	Enterocyte	Brain	Spleen	Muscle	Rest of body
V (L)	5.3	0.31	1.8	1.7	0.12	1.45	0.15	29	–[a]
Q (L/h)	356.31[b]	79.5	25.38	54.6	21.38	46.8	11.7	66.3	–[c]
Drug					K_p				
CLB	–	0.73	0.88	1.29	–	1.51	0.79	0.70	1.11
NCLB	–	0.93	1.1	1.58	–	1.89	0.99	0.88	1.29
STI	–	2.86	3.60	5.79		7.16	3.0	2.8	6.72

[a] 70 - ΣV_T

[b] cardiac output

[c] CO - ΣQ_T

Table II System Parameter Values Used in the PBPK for Clobazam (CLB) and Norclobazam (NCLB) [22]

Parameter	Description	Value
Sca_{3A4} $nmol/gut$	Total gut scaling factor for CYP3A4	66.2
Sca_{2C19} $nmol/gut$	Total gut scaling factor for CYP2C19	1.5
Ab_{3A4} $pmol\,P450/mg\,protein$	Hepatic enzyme abundance for CYP3A4	137
Ab_{2C19} $pmol\,P450/mg\,protein$	Hepatic enzyme abundance for CYP2C19	14
Ab_{2B6} $pmol\,P450/mg\,protein$	Hepatic enzyme abundance for CYP2B6	17
$ISEF_{3A4}$	Intersystem extrapolation factor for CYP3A4	0.24
$ISEF_{2C19}$	Intersystem extrapolation factor for CYP2C19	0.24
$ISEF_{2B6}$	Intersystem extrapolation factor for CYP2B6	0.43
$MPPGL\,(mg/g)$	Milligram protein per gram of liver	39.79
$LW\,(g)$	Liver weight	1,600

empirical scaling factor for CLB, $Vmax$ is the maximum metabolic velocity and Km is the Michaelis-Menten constant. $ISEF$ is a parameter that is used to scale activity per unit of enzyme in recombinant system to human liver microsomes.

The conversion of CLB to NCLB in the liver is by CYP3A4, CYP2C19 and CYP2B6 and the hepatic intrinsic clearance of CLB (the formation clearance of NCLB) in the liver is given by

$$Clint, hep(CLB)$$

$$= ESF_{CLB} \cdot \sum_i \frac{Vmax_i}{Km_i} \cdot ISEF_i \cdot Ab_i \cdot MPPGL \cdot LW \quad (3)$$

where $i = CYP3A4, CYP2C19$ and $CYP2B6$, Ab is the enzyme abundance, $MPPGL$ is the milligram protein per gram of liver and LW is the liver weight.

The conversion of NCLB to OH-NCLB in the gut and liver is by CYP2C19 only. The intrinsic clearances of NCLB in the gut and the liver are given by

$$Clint, gut(NCLB)$$

$$= ESF_{NCLB} \cdot \frac{Vmax_{2C19}}{Km_{2C19}} \cdot ISEF_{2C19} \cdot Sca_{2C19} \quad (4)$$

Table III Drugs Specific Parameter Values Used for Describing the Kinetics of Clobazam (CLB), Norclobazam (NCLB) and Stiripentol (STI)

Parameter	Description	CLB	NCLB	STI	References
MW (g)	Molecular weight	300.74	286.71	234.29	–
fu	Plasma fraction unbound	0.13	0.3	0.01	Greenblatt [8], Lundbeck [48], Levy [12]
B/P	Blood/plasma concentration ratio	1*	1*	0.58	Levy [12]
fa	Fraction absorbed from the gut	0.87	–	0.82	Rupp [47], Moreland [10]
ka (h^{-1})	Absorption rate constant	1.8	–	–	Greenblatt [8]
Vss (L)	Volume of distribution at steady state	63	–	235	Ochs [33], Chhun [11]
CL (L/h)	*In vivo* clearance	1.98	1.09	–	Greenblatt [8], Pullar [45]
CL_R (L/h)	Renal clearance	0.05	0.08	–	Volz [49], Pullar [45]
Vmax (3A4) (nmol/min/nmol P450)	Maximum metabolic velocity	6.2	–	–	Giraud [7]
Km (3A4) (μM)	Michaelis-Menten constants	29	–	–	Giraud [7]
Vmax (2C19) (nmol/min/nmol P450)	Maximum metabolic velocity	1.15	0.22	–	Giraud [7]
Km (2C19) (μM)	Michaelis-Menten constants	31.9	5.74	–	Giraud [7]
Vmax (2B6) (nmol/min/nmol P450)	Maximum metabolic velocity	5.70	–	–	Giraud [7]
Km (2B6) (μM)	Michaelis-Menten constants	289	–	–	Giraud [7]
Ki (μM) (3A4)	Inhibition constant	1.59	–	–	Giraud [13]
Ki (μM) (2C19)	Inhibition constant	0.52	0.14	–	Giraud [13]

*assumed

and

$Clint, hep(NCLB)$

$$= ESF_{NCLB} \cdot \frac{Vmax_{2C19}}{Km_{2C19}} \cdot ISEF_{2C19} \cdot Ab_{2C19} \cdot MPPGL \cdot LW \tag{5}$$

Vmax and *Km* values for the enzymes involved in the metabolism of CLB and NCLB have been determined by Giraud *et al.* [7] in recombinant systems (Table III) and were used in the equations above to predict the intrinsic clearances of CLB and NCLB. Other system parameters such as *ISEF*, *Ab*, *MPPGL* and *Sca* were set to default values used in the program Simcyp [22]. *ESF* parameters were set to values that allow CLB and NCLB clearances to match *in vivo* values.

Stiripentol

Due to lack of information in the literature on the characterisation of the metabolism of STI in *in vitro* systems, parameters for the clearance of STI were estimated. From an *in vivo* study involving healthy volunteers, 18 metabolites of STI were identified in urine and these along with the parent compound accounted for more than 70% of the administered dose [4, 10]. Most these metabolites were formed by the opening of the methylenedioxy ring to generate catechol derivatives. It has also been suggested that the metabolites are not detectable in plasma because they exist as conjugates and are subsequently excreted into urine as conjugates [12]. For compounds in this structural class, it has been suggested that conversion of the methylenedioxy ring to its catechol derivatives is catalysed by cytochrome P-450 enzymes [10]. CYP1A2, CYP2C19 and CYP3A4 have been suggested as the Phase I enzymes involved in the metabolism of STI based on *in vitro* studies [4]. However no data is available in the literature on the contribution of each of these enzymes and other parameters necessary for *in vitro-in vivo* extrapolation (IVIVE). Plasma concentration data from *in vivo* studies have shown that STI exhibit nonlinear kinetics, Levy *et al.* and others [11, 12, 15, 23, 24] have reported Michaelis-Menten kinetics for STI in humans. It has also been shown that single dose kinetic data does not predict steady state plasma concentration levels [12]. In this current study, elimination of STI was therefore described using a Michaelis-Menten kinetic model and the parameters (*Vmax* and *Km*) were estimated by fitting the PBPK model to plasma concentration data obtained from the literature, assuming the liver is the main organ responsible for elimination. Also different *Vmax* parameters were assumed for single and chronic dosing to account for time-dependence in the PK of STI that has been reported in the literature [12]. The fitting was carried out using the NONMEM software using a naïve pooled data approach [25]. The data used for the fitting

included data obtained following single and chronic dosing of STI in healthy volunteers. The single dose data was obtained from an individual after doses of 300 mg, 600 mg and 1,200 mg on three different occasions [12]. The steady state data was obtained from two individuals who received STI three times a day for 14 days using three dosage increments: 600 mg/day (3 days), 1,200 mg/day (4 days) and 1,800 mg/day (7 days). Nine samples, each separated by 1 h were collected on days 3, 7 and 18 [23].

Clobazam/Norclobazam and STI interaction

The metabolic interaction between STI and CLB/NCLB which has been studied using both *in vitro* and *in vivo* experiments was incorporated in the PBPK model [13, 14]. Giraud *et al.* [13] investigated the inhibitory effect of STI on CLB/NCLB metabolism mediated by CYP3A4 and CYP2C19 enzymes using recombinant system. The mechanism of interaction and the inhibition constant (*Ki*) reported were incorporated into the PBPK model.

Scaling

The PBPK models developed for adults were scaled to children assuming pathways for drug metabolism are the same in adults and children. Benzodiazepines are known to bind to albumin in plasma, and therefore binding to albumin was assumed for CLB and NCLB [26]. Plasma protein binding was adjusted in children using the equations proposed by McNamara and Alcorn [27]. Age related changes in albumin levels in children were predicted using the equation proposed by Johnson *et al.* [19]. For STI the same binding parameter estimate was assumed in children and adults due to lack of information in the literature on the plasma protein it binds to. Enzyme abundance (CYP3A4 and CYP2C19 in the gut and CYP3A4, CYP2C19 and CYP2B6 in the liver) were adjusted for CLB and NCLB clearance prediction in children using the equations proposed by Salem *et al.* [28]. Renal clearance was scaled to children using GFR. Reference values for GFR at different paediatric age groups were obtained from the data published by Johnson *et al.* [19]. The hepatic intrinsic *Vmax* for STI was scaled to children by using allometry [29].

Variability

Variability on drug and system parameters was introduced in the PBPK model, allowing simulated and observed plasma concentration data to be comparable both in terms of the mean profile and variability. Variability in the simulations was mainly due to variability on BW and BSA. Variability on BW propagates in the simulation through organs/tissue volumes while variabilities on HT and WT propagate through cardiac output and therefore through organ/tissue blood flows. Other

drug and system parameters with variability are GFR, HT, ka, fa, Sca, K_p, fu, CL_R, $Vmax$ and km. A lognormal distribution was assumed for all parameters and a CV of 15% was used.

Simulation

The PBPK model was used to simulate plasma concentration profiles following single and chronic dosing of CLB and STI both in adults and children. Simulated plasma concentration profiles were compared with observed data reported in the literature for the drugs to allow assessment of the model. In all cases, attempts were made to match data used for simulations with the reported data in the publications especially in terms of age and dose. Simulations were performed for a virtual population of 1,000 subjects in all cases and 2.5th, 50th and 97.5th percentiles were determined and plotted together with observed plasma concentration data. In some cases individual plasma concentration data or mean and standard deviation or standard error were reported, whereas in other cases individual profiles or population mean profiles with standard deviation or standard error bars were reported in figures. For the latter, the data were digitized using GetData Graph Digitizer [30]. The interaction between STI and CLB and NCLB was also incorporated in some of the simulations and the extent of the interaction at different paediatric age groups was simulated. The differential equations that describe changes in plasma and tissue concentrations were implemented in MATLAB software [31] and also used for simulations.

RESULTS

Parameter estimates in Tables I, II, III and IV for system and drug specific parameters were utilised in the PBPK model. Table IV shows the parameter estimates and the percentage relative standard errors ($SE\%$) obtained from fitting the PBPK to STI plasma concentration data obtained from the literature using NONMEM. All the parameters were well estimated as the $SE\%$ are below 20% for all parameters. As expected the maximum metabolic rate parameter, Vmax

estimated following single (Vmax, s) and chronic (Vmax, c) dosing were significantly different. The enzyme(s) responsible for the metabolism appears to have lost more than 50% of the activity following chronic dosing. The simulated median plasma and tissue profiles for CLB, NCLB and STI following oral single dose of CLB (30 mg) and STI (300 mg) in adults are shown in Fig. 2. For CLB, following a very rapid absorption, the plasma profile fall mono-exponentially and the profiles for other tissues such as the gut, kidney, liver, brain, spleen, muscle and the rest of body are parallel to plasma profile. The highest C_{max} of CLB is achieved in the brain out of all the tissues/organs. The profiles for NCLB in the tissues follow the same pattern as CLB, however C_{max} of NCLB is achieved much later in all the tissues compared to CLB. Also $t_{1/2}$ of NCLB is longer than CLB in all the tissues. For STI, a rapid absorption is followed by a biphasic decline of the profiles in all tissues especially in plasma; an initial rapid decline is followed by a slower decline. The highest C_{max} is achieved in the liver compared to all tissues and the $t_{1/2}$ of the drug appears to be longer in the rest of body, which is consistent with a very large volume of distribution for the drug, which has been observed with *in vivo* data [11].

Figure 3 shows normalised simulated plasma concentration profiles (2.5th, 50th and 97.5th percentiles) with the observed plasma concentration data of CLB and NCLB following single dose (10, 20, 30 and 40 mg) administration of CLB in adults. Individual data were obtained from multiple sources; 10 mg data was obtained from Tedeschi *et al.* [32], 20 mg that data was obtained from Ochs *et al.* [33], Greenblatt [34], Divoll *et al.* [35], Greenblatt *et al.* [6], Bun *et al.* [36], and Greenblatt *et al.* [37], 30 mg data was obtained from Pullar *et al.* [38] and Jawad *et al.* [39] and 40 mg data was obtained from Vallner *et al.* [40]. All these data were dose normalised. In the figure, 95% prediction interval appears to under-predict the variability in CLB data, whereas the interval appears to be satisfactory for NCLB. While the median profile appears to be satisfactory for CLB, it appears to over-predict the observed data for NCLB.

Figure 4 shows simulated plasma concentration profiles (2.5th, 50th and 97.5th percentiles) superimposed with mean observed plasma concentration data and standard deviation bars of CLB and NCLB following chronic dosing of CLB in

Table IV Parameters Values Estimated for Stiripentol (STI) Following Fitting of the PBPK Model to Plasma Profiles

Parameter	Description	Estimate	SE (%)[a]
Vmax, s (mg/h)	Maximum metabolic velocity (single dose)	270	13
Vmax, m (mg/h)	Maximum metabolic velocity (multiple dose)	118	8
Km (mg/L)	Michaelis-Menten constant	0.03	15
ka ($/h$)	Absorption rate constant	0.58	13

[a] Percentage relative standard error

Fig. 2 Simulated median plasma and tissue concentration of clobazam (CLB), norclobazam (NCLB) and stiripentol (STI) in adults following oral single dose administration of 30 mg CLB and 300 mg STI.
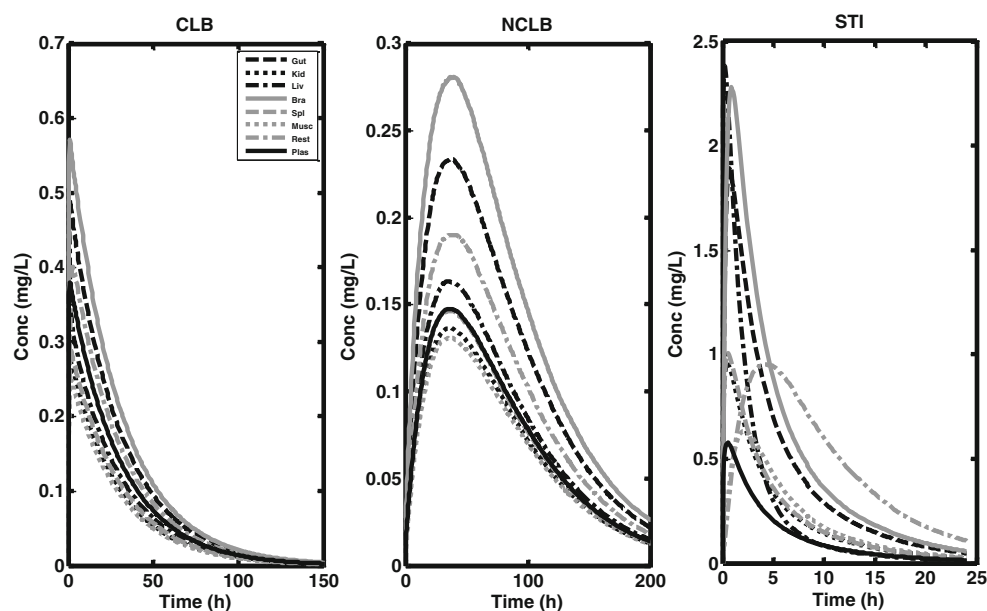

adults [33]. The data was obtained from nine healthy volunteers that received 5 mg CLB twice daily for 22 consecutive days. The prediction interval shows adequate coverage of the data both for CLB and NCLB and the simulations therefore reflect the mean observed profile and the variability in the data. Figure 5 also shows simulated 95% prediction interval and the median profiles superimposed with the mean observed plasma concentration data for CLB and NCLB following chronic dosing of CLB in adults [36]. In the study, six healthy volunteers received 10 mg of CLB twice daily for 28 consecutive days. Only the mean data was reported in the publication and the model prediction of CLB concentrations shows slight over-prediction, while that of NCLB shows slight under-prediction.

Figure 6 shows simulated plasma concentration profiles (2.5th, 50th and 97.5th percentiles) and the observed plasma concentration data in an adult following three single doses of STI on different occasions [12]. The data in the plots was part of the data used for fitting to estimate some drug specific parameters for STI, especially the parameters that describe

Fig. 3 Normalised simulated plasma concentration profiles (2.5th, 50th and 97.5th percentiles) and observed plasma concentration data with the median profiles for clobazam (CLB) and norclobazam (NCLB) following oral single dose (10, 20, 30 and 40 mg) administration of CLB in adults.
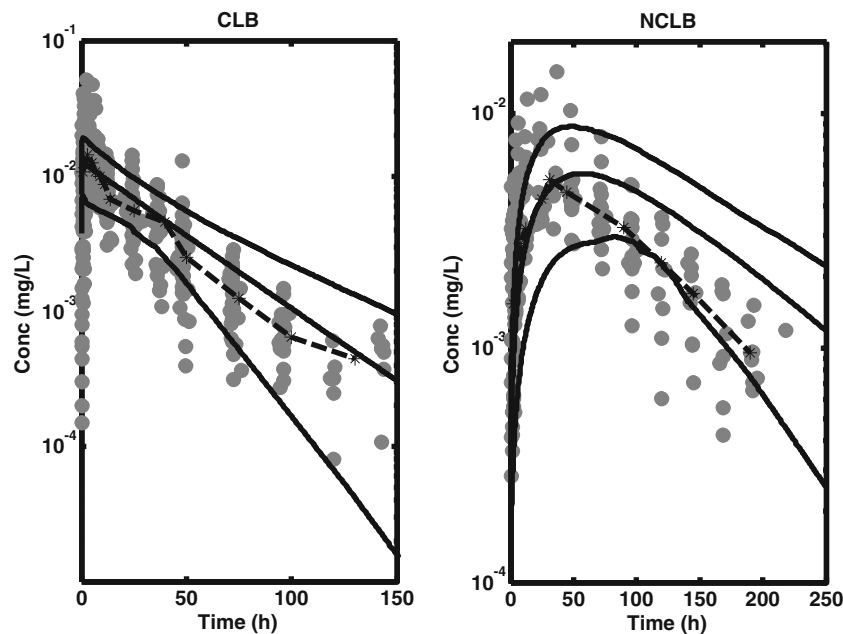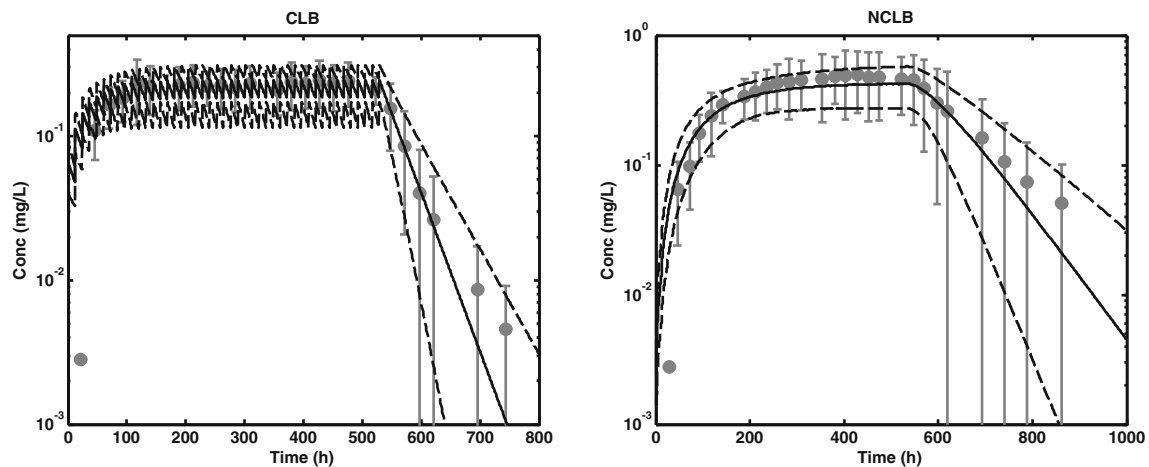
Fig. 4 Simulated plasma concentration profiles (2.5th, 50th and 97.5th percentiles) and observed mean plasma concentration with standard deviation *bars* of clobazam (CLB) and norclobazam (NCLB) following chronic oral dosing of CLB in adults (Ochs *et al*. [33]).

the nonlinear elimination. The median profiles in the plots can therefore be seen as fitted lines and the prediction intervals are based on simulations using these parameters and other parameters with variability incorporated on all parameters. Figure 7 shows simulated plasma concentration profiles (2.5th, 50th and 97.5th percentiles) and the observed plasma concentration data in an adult following chronic dosing of STI in three dosage increments [23]. The data in the plots was also part of the data used for parameter estimation and the median line is therefore a fitted line.

Figure 8 shows simulated plasma concentration profiles and the observed mean plasma concentration data (with standard deviation bars) in healthy volunteers (adults) on oral STI for 13 days in three incremental doses i.e. 500 mg twice daily (1 day), 1,000 mg twice daily (1 day) and 1,500 mg twice daily (11 days) [14]. Twelve subjects were enrolled in the study and

minimum plasma concentration (C_{min}) was determined on days 11, 12 and 13. The model satisfactorily predicts the mean C_{min} but over-predicts the variability in the data. Figure 9 shows simulated plasma concentration profiles and the observed trough plasma concentration data (with standard deviation bars) in three different age groups including children and adults following chronic oral dosing of STI. May *et al*. [41] provides detailed information on the experimental settings, demographic data, STI doses and plasma concentration observed in the different age groups. Only one data point for each age group was reported in the publication as shown in the plots. In all age groups, the model appears to slightly overpredict the trough concentration and the variability in the data.

Figures 10 and 11 show simulated median plasma concentration profiles for CLB and NCLB and simulated plasma
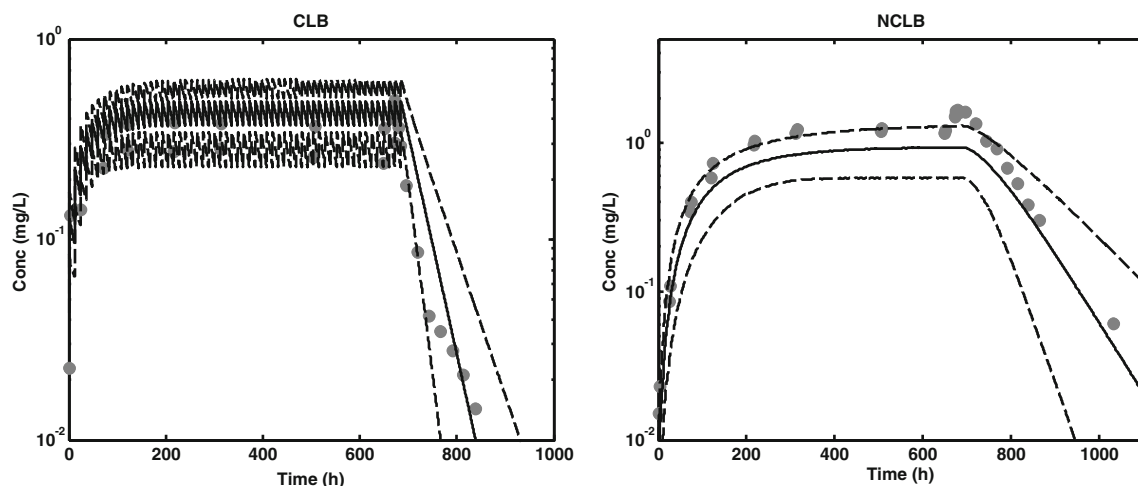

Fig. 5 Simulated plasma concentration profiles (2.5th, 50th and 97.5th percentiles) and observed mean plasma concentration of clobazam (CLB) and norclobazam (NCLB) following chronic oral dosing of CLB in adults (Bun *et al*. [36]).

Fig. 6 Simulated plasma concentration profiles (2.5th, 50th and 97.5th percentiles) and observed plasma concentration of stiripentol (STI) following single oral doses (Levy *et al.* [12]).
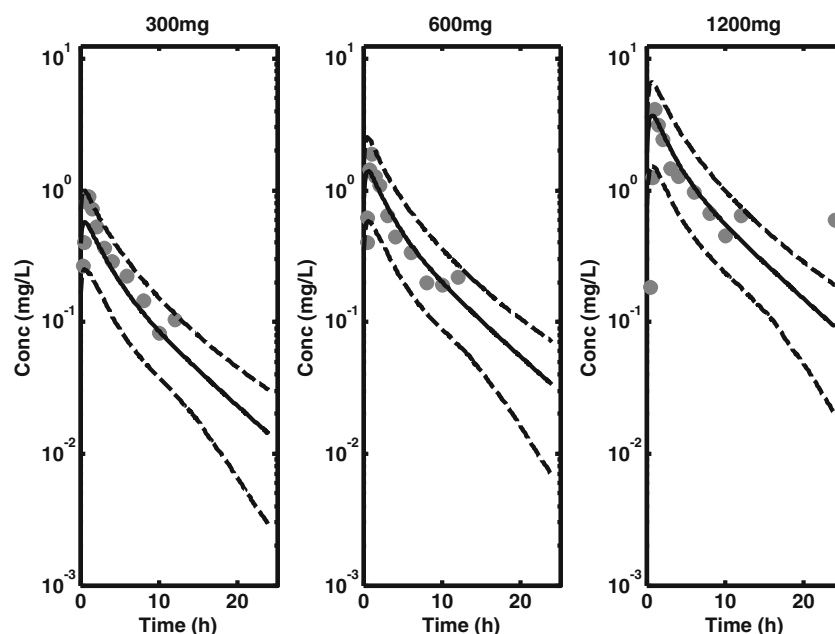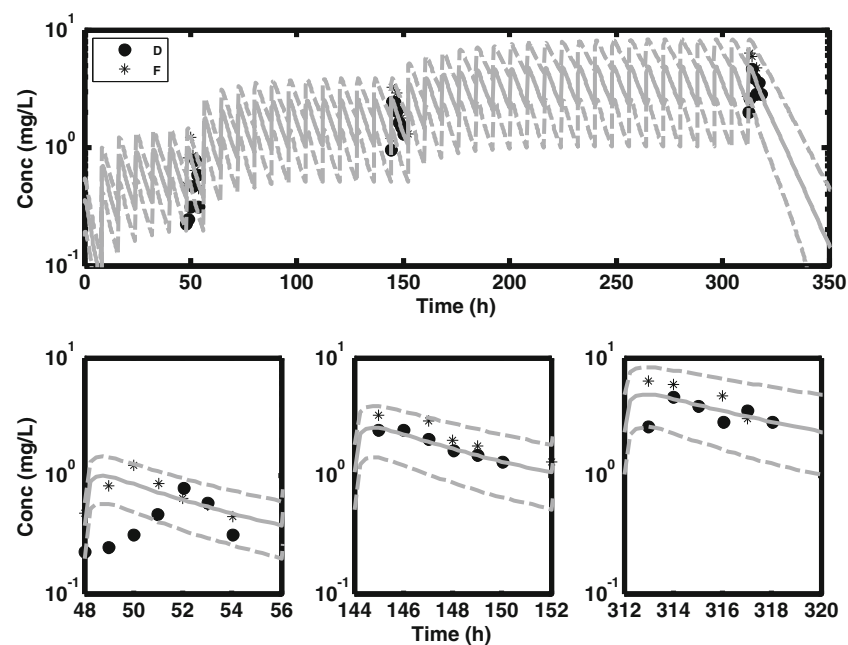

concentration profiles (2.5th, 50th and 97.5th percentiles) for STI for different paediatric age groups and adults following chronic dosing of CLB and STI. Figure 10 shows the effect of STI on the inhibition of the metabolism of CLB and NCLB, the simulations were based on oral administration of 0.5 mg/kg/day and 50 mg/kg/day for CLB and STI respectively for 28 days. The plots show that C_{max} of CLB and NCLB in the presence and absence of STI increases with age. The effect of STI is more pronounced on NCLB compared to CLB. The effect of STI on CLB is more pronounced in adults

compared to other age groups while the effect of STI on NCLB is more pronounced in the 12 years old compared to other age groups. STI profiles in Fig. 11 shows that the highest C_{max} is observed in adults, the non-linearity in the metabolism of STI appears to be more pronounced as age increases thereby leading to more accumulation of the drug. Also, the variability in the simulation appears to be more pronounced as age increases.

The plots in Fig. 12 show the effect of STI on CLB and NCLB as observed in a clinical study in children (3–16.7 years)

Fig. 7 Simulated plasma concentration profiles (2.5th, 50th and 97.5th percentiles) and observed plasma concentration of stiripentol (STI) following chronic oral dosing in adults (Levy *et al.* [23]).
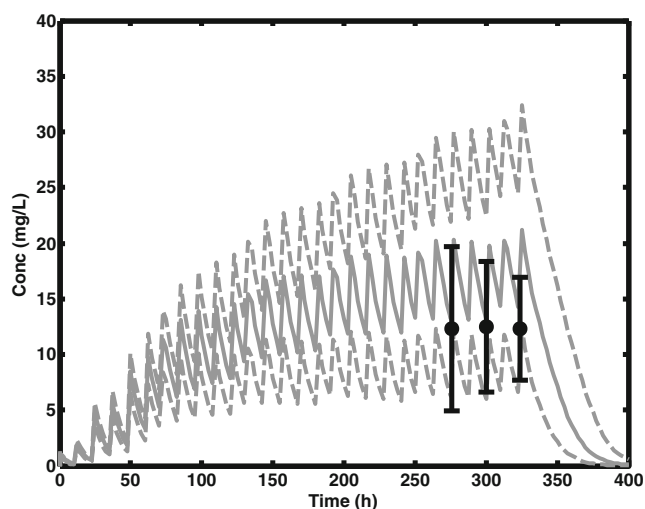
Fig. 8 Simulated plasma concentration profiles (2.5th, 50th and 97.5th percentiles) and observed mean plasma concentration with standard deviation *bars* of stiripentol (STI) following chronic oral dosing in adults (Tran *et al.* [14]).

of CLB and STI. The study was carried out in SMEI who received CLB and STI twice or thrice daily for a month. Chiron *et al.* (5) presented the details of the study which was designed to show the efficacy of STI as an add-on therapy in the treatment of SMEI. The predicted and the observed C_{min} of STI in the children (mean and 95% confidence interval) were 10.12 mg/L (2.51–39.36 mg/L) and 10.0 mg/L (8.3–11.7 mg/L) respectively. For CLB alone the predicted and the observed C_{min} were 0.19 mg/L (0.05–0.49 mg/L) and 0.20 mg/L (0.17–0.23 mg/L) respectively and for NCLB the predicted and the observed C_{min} were 0.49 mg/L (0.16–1.38 mg/L) and 0.95 mg/L (0.91–0.99 mg/L) respectively. For CLB (including interaction with STI) the predicted and observed C_{min} were 0.29 mg/L (0.07–1.05 mg/L) and 0.31 mg/L (0.24–0.38 mg/L) respectively and for NCLB the predicted and the observed C_{min} were 2.30 mg/L (0.45–5.53 mg/L) and 4.32 mg/L (3.77–4.87 mg/L) respectively. The results show that the model adequately predicts CLB mean C_{min} with and without interaction with STI, but for NCLB the mean C_{min} is under-predicted with and without interaction. The mean C_{min} for STI is also adequately predicted. In all cases i.e. CLB and NCLB with and without interaction and STI, the variability in the data is under-predicted although the observed variability for CLB, NCLB and STI in the study is much lower than what has been reported in the literature for other clinical studies [42, 43].
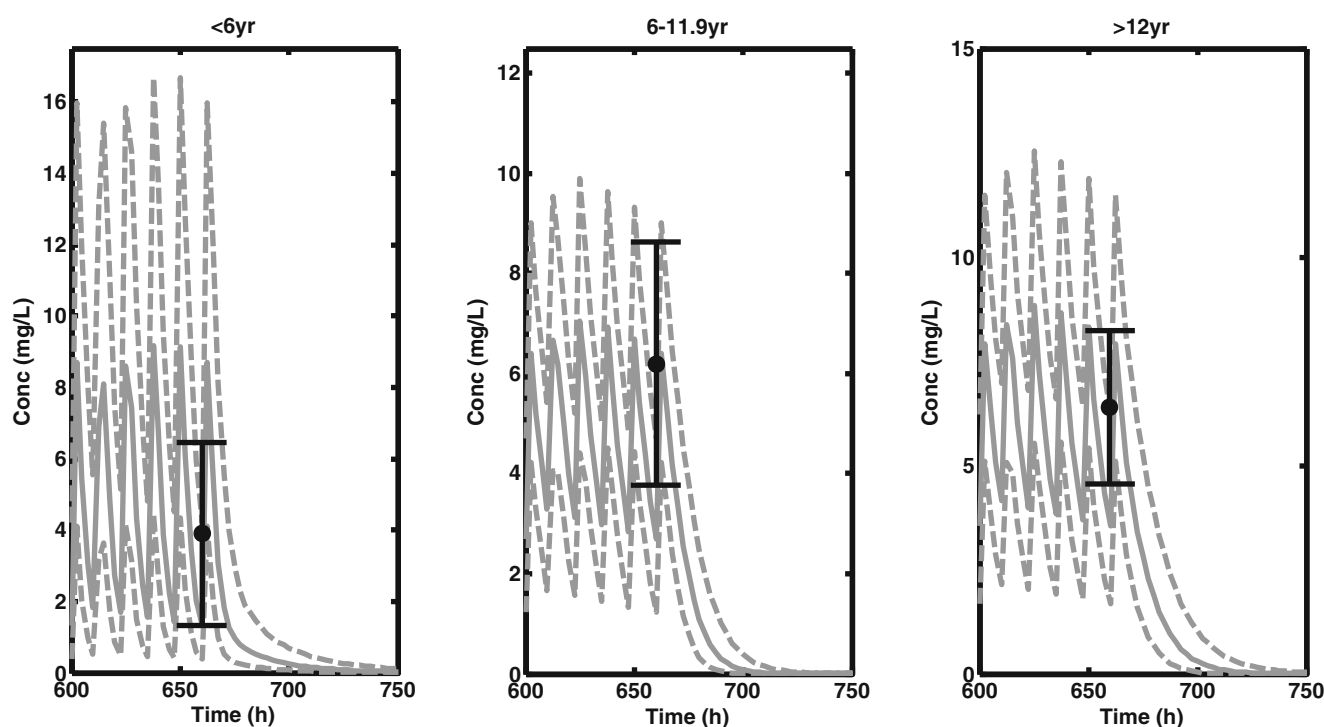
where CLB was administered alone and co-administered with STI. The plots show 95% prediction intervals and median profiles of CLB and NCLB with and without interaction with STI. Also superimposed on these are the reported mean plasma C_{min} (and the 95% confidence interval bars) during one dosing interval after several doses

Fig. 9 Simulated plasma concentration profiles (2.5th, 50th and 97.5th percentiles) and observed mean plasma concentration with standard deviation *bars* of stiripentol (STI) following chronic oral dosing in children and adults (May *et al.* [41]).
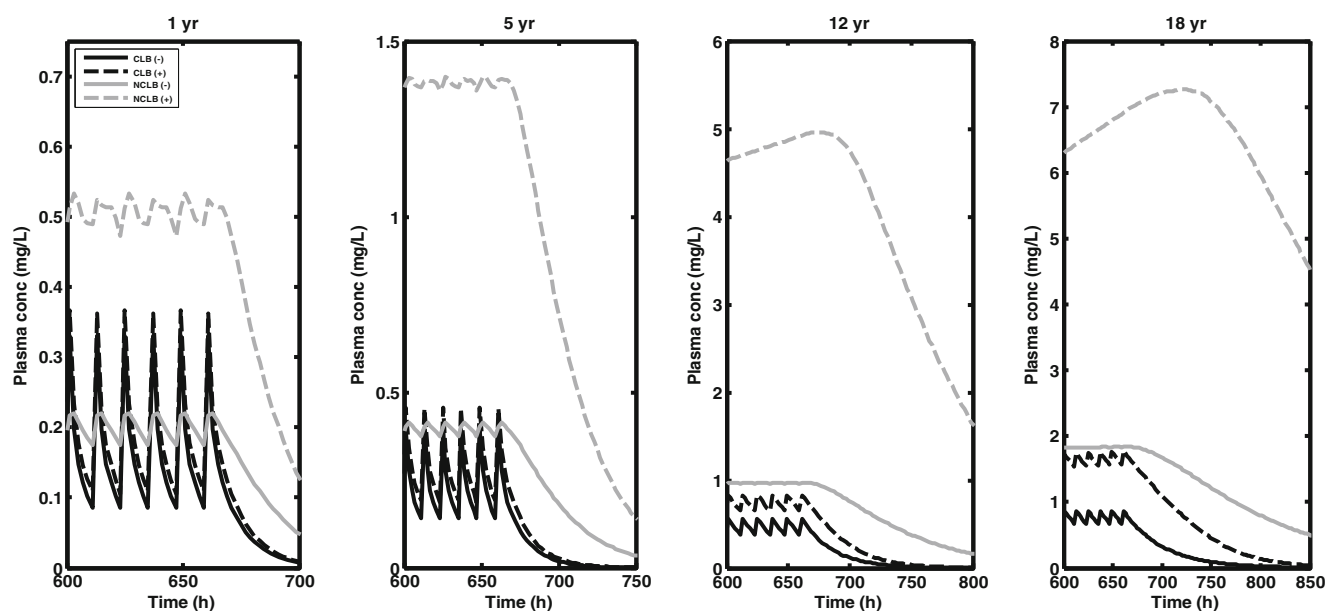
Fig. 10 Simulated median plasma concentration profiles of clobazam (CLB) and norclobazam (NCLB) in different paediatric age groups and adults following chronic oral dosing of CLB and stiripentol (STI) (simulations include interaction between CLB/NCLB and STI).

DISCUSSION

This work has developed a PBPK model for the purpose of predicting plasma and tissue concentration in adults and children following acute and chronic dosing of CLB and STI. The work forms part of a project that is dedicated to the use of modelling and simulation in the evaluation of treatments for rare diseases in children. In this case the disease

is DS and the treatment includes CLB, STI and VPA. The focus of this work is on CLB and STI and the main objective was to develop PBPK models that predict tissue concentrations, especially brain, so that this can be linked with disease model that is being developed in another part of the project to produce a PBPK-PD model that is capable of simulating clinical trial outcomes. CLB is metabolised to an active metabolite, NCLB that has a longer $t_{1/2}$ and achieve a higher
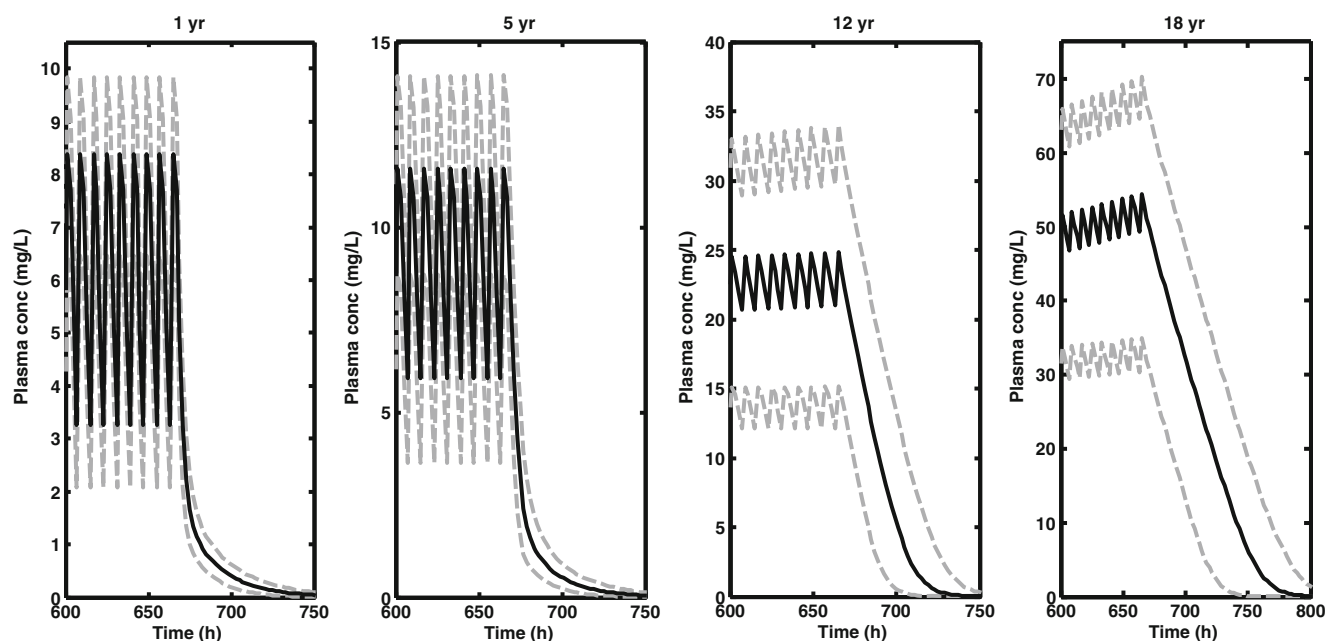

Fig. 11 Simulated median plasma concentration profiles of stiripentol (STI) in different paediatric age groups and adults following chronic oral dosing of clobazam (CLB) and STI.
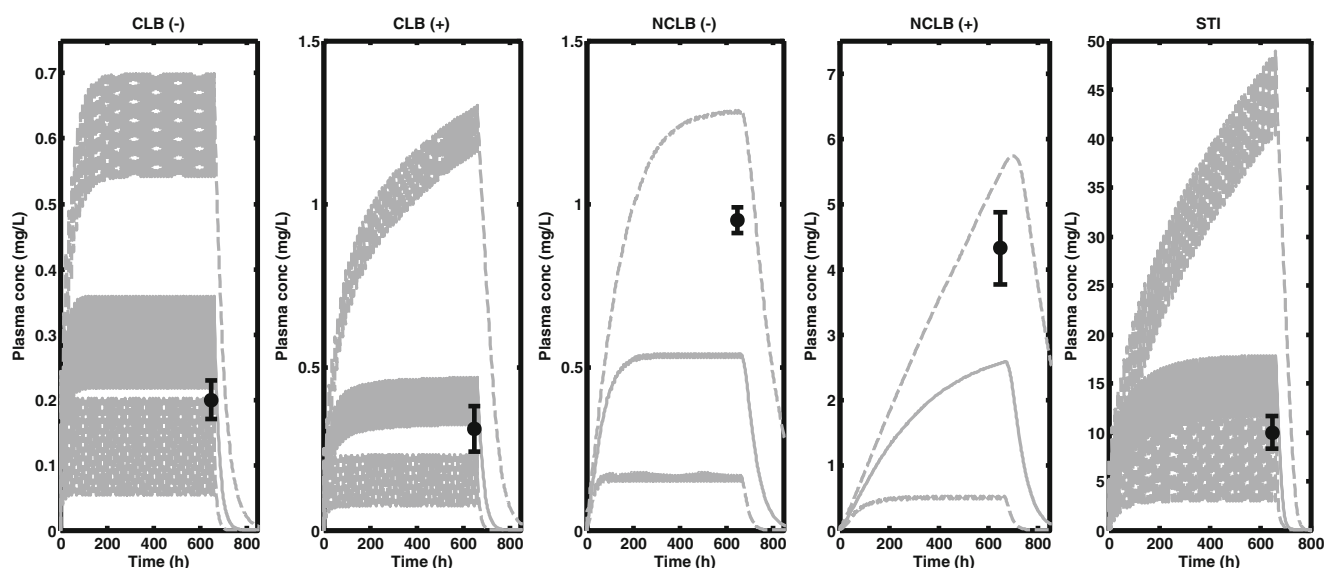
Fig. 12 Simulated plasma concentration profiles (2.5th, 50th and 97.5th percentiles) and observed mean plasma concentration with standard deviation *bars* of clobazam (CLB), nordobazam (NCLB) and stiripentol (STI) following chronic oral dosing of CLB and STI in children (Chiron *et al.* [5], (−) simulations without interaction and (+) simulations with interaction between CLB/NCLB and STI).

concentration following chronic dosing and has been suggested to be more important for the efficacy of CLB following long term dosing. It is therefore important that this metabolite is accounted for in the model developed for CLB. The model also incorporates the reported PK interaction that has been demonstrated between CLB/NCLB and STI both in *in vitro* and *in vivo* systems. It has been demonstrated that STI is a potent inhibitor of several CYP450 enzymes and this has been suggested as the rationale for its success as an add-on therapy in the treatment of DS. The approach that has been followed in this work is to develop and validate a PBPK model in adults, which is then scaled to children using age-dependent anatomical and physiological information in children. This is similar to a workflow that was published recently for developing a PBPK model to support paediatric research and development using Lorazepam as a case study [44].

The PBPK model developed for CLB/NCLB and STI has compartments for gut lumen, enterocyte, gut tissue, systemic blood, kidney, liver, brain, spleen, muscle and rest of body. The data used for model building and validation were obtained from the literature: both *in vitro-in vivo* extrapolation (IVIVE) and parameter estimation techniques were used. PBPK models based on IVIVE techniques have been widely used to describe the PK of drugs and in this work this was applied to CLB and NCLB. However in the case of STI due to lack of information in the literature on the *in vitro* characterisation of STI metabolism, parameter estimation was used based on information in the literature. $K_p s$ are a very important component of PBPK models that help to explain how the drug distribute into different tissues. A number of equations have been developed to predict $K_p s$ when experimentally

determined values in preclinical species such as rat, mice, rabbits, dogs, monkeys etc. are not available. These equations require input parameters such as the physicochemical properties and plasma protein binding of the drug. In this study the equation proposed by Rodgers *et al.* [20, 21] has been used to predict $K_p s$ for different tissues and the $K_p s$ for the rest of body compartment was obtained by lumping other tissues/organs that have not been accounted for explicitly in the model. The predicted volume of distribution at steady state (V_{SS}) using the $K_p s$ were 0.85 L/kg, 0.99 L/kg and 2.2 L/kg for CLB, NCLB and STI respectively. The observed V_{SS} were 0.9 L/kg (male), 1.10 L/kg (female), 0.87 L/kg (young male), 1.4 L/kg (young female), 1.4 L/kg (elderly male) and 1.8 L/kg (elderly female) for CLB [8, 33]. For STI the observed volume of distribution is around 3 L/kg [4]. These show that the distribution of CLB and NCLB are limited to highly perfused tissues while STI tends to distribute to some extent to adipose and other related tissues. This is also portrayed in the profiles of the drugs in Fig. 2 with CLB and NCLB showing monophasic decline and STI showing a biphasic decline.

The clearance of CLB and NCLB used in the PBPK model was extrapolated from *in vitro* parameters that have been obtained from previous experiment that was used to characterise their metabolism. However ESF were also needed to recover the observed plasma concentration profiles for both CLB and NCLB. While the intrinsic clearance obtained was too high for CLB, it was too low for NCLB. The reported *in vivo* oral clearance (CL/F) in the literature for CLB and NCLB are approximately 1.9 and 1.1 L/h respectively, with the bioavailability of CLB reported to be up to 0.87 [8, 32, 33,

35, 38–40, 45–47]. The hepatic intrinsic clearance of CLB ($Clint, hep(CLB)$) and NCLB ($Clint, hep(NCLB)$) calculated using Eqs. 3 and 5 above and then scaled using the well stirred model gave hepatic metabolic clearances in blood of 3.48 L/h and 0.15 L/h for CLB and NCLB respectively without ESF. However when ESF were included in the equations, the hepatic metabolic clearance in blood were 2.12 L/h and 1.58 L/h for CLB and NCLB respectively. It is not clear why it is not possible to recover the intrinsic clearance from *in vitro* parameters or why the system is inconsistent for CLB and NCLB. However it is not unusual in PBPK modelling based on IVIVE to use *in vivo* experimental values to recover observed values. Due to lack of information in the literature, it was not possible to use IVIVE technique to describe the PK of STI and therefore estimates for some parameters in the PBPK model were obtained through parameter estimation. STI is an orphan drug and it is therefore not surprising that there are gaps in the information that is available in the literature. $Vmax$, Km and ka were estimated from fitting the PBPK model to plasma concentration data that have been reported in the literature following single and multiple doses. Because it has been shown that single dose kinetic data does not predict steady state plasma concentration levels, different $Vmax$ estimates were obtained for single and steady state data. The estimates obtained for the two parameters were significantly different possibly suggesting loss of activity by the enzyme involved in the metabolism following chronic dosing. This suggests possible time-dependent inhibition of the enzyme or some other mechanism such as product inhibition that can lead to reduce activity following chronic dosing of a drug. Tran *et al.* [14] from their work concluded that STI did not appear to be a mechanism based inhibitor, but with the limited amount of evidence in the literature on the accumulation of STI at steady state this needs to be further investigated in order to have a better understanding of the PK of STI especially following chronic dosing. Also an important limitation of this work is the amount of data used to estimate $Vmax$, Km and ka for STI. These parameters therefore need further validation using a larger data set or this part of the model replaced with IVIVE information once the metabolism of STI is fully characterised.

CONCLUSION

A PBPK model that describes the PK of CLB, NCLB and STI has been developed based on IVIVE extrapolation and parameter estimation techniques. The model incorporates a clinically significant interaction that has been reported for CLB/NCLB and STI. The model can be used to simulate plasma and tissue concentrations in both adults and children following oral dosing of CLB and STI and should help to improve the use of CLB and STI in the treatment of patients with DS.

REFERENCES

1. Hurst DL. Epidemiology of severe myoclonic epilepsy of infancy. Epilepsia. 1990;31:397–400.
2. Morse RP. Dravet syndrome: inroads into understanding epileptic encephalopathies. J Pediatr. 2011;158:354–9.
3. Chiron C, Dulac O. The pharmacologic treatment of Dravet syndrome. Epilepsia. 2011;52 Suppl 2:72–5.
4. Plosker GL. Stiripentol: in severe myoclonic epilepsy of infancy (dravet syndrome). CNS Drugs. 2012;26:993–1001.
5. Chiron C, Marchand MC, Tran A, Rey E, Athis P, Vincent J, *et al.* Stiripentol in severe myoclonic epilepsy in infancy: a randomised placebo-controlled syndrome-dedicated trial. STICLO study group. Lancet. 2000;356:1638–42.
6. Greenblatt DJ, Divoll M, Abernethy DR, Ochs HR, Shader RI. Clinical pharmacokinetics of the newer benzodiazepines. Clin Pharmacokinet. 1983;8:233–52.
7. Giraud C, Tran A, Rey E, Vincent J, Treluyer JM, Pons G. *In vitro* characterization of clobazam metabolism by recombinant cytochrome P450 enzymes: importance of CYP2C19. Drug Metab Dispos. 2004;32:1279–86.
8. Greenblatt DJ, Divoll M, Puri SK, Ho I, Zinny MA, Shader RI. Clobazam kinetics in the elderly. Br J Clin Pharmacol. 1981;12:631–6.
9. Chiron C. Stiripentol Neurother. 2007;4:123–5.
10. Moreland TA, Astoin J, Lepage F, Tombret F, Levy RH, Baillie TA. The metabolic fate of stiripentol in man. Drug Metab Dispos. 1986;14:654–62.
11. Chhun S, Peigne S, Rey E, Pons G, Jullien V. Population pharmacokinetic study in healthy volunteers treated with 3 single doses of stiripentol (500, 1,000, 2,000 mg). Fundam Clin Pharmacol. 2009;23:24–5.
12. Levy RH, Lin HS, Blehaut HM, Tor JA. Pharmacokinetics of stiripentol in normal man: evidence of nonlinearity. J Clin Pharmacol. 1983;23:523–33.

13. Giraud C, Treluyer JM, Rey E, Chiron C, Vincent J, Pons G, *et al*. *In vitro* and *in vivo* inhibitory effect of stiripentol on clobazam metabolism. Drug Metab Dispos. 2006;34:608–11.

14. Tran A, Rey E, Pons G, Rousseau M, d'Athis P, Olive G, *et al*. Influence of stiripentol on cytochrome P450-mediated metabolic pathways in humans: *in vitro* and *in vivo* comparison and calculation of *in vivo* inhibition constants. Clin Pharmacol Ther. 1997;62:490–504.

15. Levy RH, Loiseau P, Guyot M, Blehaut HM, Tor J, Moreland TA. Stiripentol kinetics in epilepsy: nonlinearity and interactions. Clin Pharmacol Ther. 1984;36:661–9.

16. Valentin J. Basic anatomical and physiological data for use in radiological protection: reference values: ICRP Publication 89. Ann ICRP. 2002;32:1–277.

17. Haycock GB, Schwartz GJ, Wisotsky DH. Geometric method for measuring body surface area: a height-weight formula validated in infants, children, and adults. J Pediatr. 1978;93:62–6.

18. DuBois D, DuBois EF. A formula to estimate the approximate surface area if height and weight be known. Arch Intern Med. 1916;17:863–71.

19. Johnson TN, Rostami-Hodjegan A, Tucker GT. Prediction of the clearance of eleven drugs and associated variability in neonates, infants and children. Clin Pharmacokinet. 2006;45:931–56.

20. Rodgers T, Rowland M. Physiologically based pharmacokinetic modelling 2: predicting the tissue distribution of acids, very weak bases, neutrals and zwitterions. J Pharm Sci. 2006;95:1238–57.

21. Rodgers T, Leahy D, Rowland M. Physiologically based pharmacokinetic modeling 1: predicting the tissue distribution of moderate-to-strong bases. J Pharm Sci. 2005;94:1259–76.

22. Jamei M, Turner D, Yang J, Neuhoff S, Polak S, Rostami-Hodjegan A, *et al*. Population-based mechanistic prediction of oral drug absorption. AAPS J. 2009;11:225–37.

23. Levy RH, Loiseau P, Guyot M, Blehaut HM, Tor J, Moreland TA. Michaelis-Menten kinetics of stiripentol in normal humans. Epilepsia. 1984;25:486–91.

24. Rey E, Jullien V, D'Athis P, Vincent J, Pons G. Is pharmacokinetics of stiripentol linear? Clin Pharmacol Ther. 2005;77:P64–4.

25. Beal S, Sheiner LB, Boeckmann A, Bauer RJ. NONMEM User's guides. (1989–2009). Ellicott City: Icon Development Solutions; 2009.

26. Menke G, Pfister P, Sauerwein S, Rietbrock I, Woodcock BG, Rietbrock N. Age-dependence and free fatty acid modulation of binding kinetics at the benzodiazepine binding site of serum albumin in neonates and adults determined using fast reaction methods. Br J Clin Pharmacol. 1987;23:439–45.

27. McNamara PJ, Alcorn J. Protein binding predictions in infants. AAPS PharmSci. 2002;4:E4.

28. Salem F, Johnson TN, Barter ZE, Leeder JS, Rostami-Hodjegan A. Age related changes in fractional elimination pathways for drugs: assessing the impact of variable ontogeny on metabolic drug-drug interactions. J Clin Pharmacol. 2013;53:857–65.

29. West GB, Brown JH, Enquist BJ. The fourth dimension of life: fractal geometry and allometric scaling of organisms. Science. 1999;284: 1677–9.

30. GetData Graph Digitizer, http://getdata-graph-digitizer.com/2013.

31. MATLAB 7.14.0.739. Natick, Massachusetts: The MathWorks Inc. R 2012a.

32. Tedeschi G, Riva R, Baruzzi A. Clobazam plasma-concentrations - pharmacokinetic study in healthy-volunteers and data in epileptic patients. Br J Clin Pharmacol. 1981;11:619–22.

33. Ochs HR, Greenblatt DJ, Luttkenhorst M, Verburg-Ochs B. Single and multiple dose kinetics of clobazam, and clinical effects during multiple dosage. Eur J Clin Pharmacol. 1984;26:499–503.

34. Greenblatt DJ. Electron-capture GLC determination of clobazam and desmethylclobazam in plasma. J Pharm Sci. 1980;69:1351–2.

35. Divoll M, Greenblatt DJ, Ciraulo DA, Puri SK, Ho I, Shader RI. Clobazam kinetics: intrasubject variability and effect of food on adsorption. J Clin Pharmacol. 1982;22:69–73.

36. Bun H, Coassolo P, Gouezo F, Serradimigni A, Cano JP. Time-dependence of clobazam and N-demethylclobazam kinetics in healthy volunteers. Int J Clin Pharmacol Ther Toxicol. 1986;24: 287–93.

37. Greenblatt DJ, Divoll M, Puri SK, Ho I, Zinny MA, Shader RI. Reduced single-dose clearance of clobazam in elderly men predicts increased multiple-dose accumulation. Clin Pharmacokinet. 1983;8: 83–94.

38. Pullar T, Edwards D, Haigh JR, Peaker S, Feely MP. The effect of cimetidine on the single dose pharmacokinetics of oral clobazam and N-desmethylclobazam. Br J Clin Pharmacol. 1987;23:317–21.

39. Jawad S, Richens A, Oxley J. Single dose pharmacokinetic study of clobazam in normal volunteers and epileptic patients. Br J Clin Pharmacol. 1984;18:873–7.

40. Vallner JJ, Kotzan JA, Stewart JT, Honigberg IL, Needham TE, Brown WJ. Plasma levels of clobazam after 10-, 20-, and 40-mg tablet doses in healthy subjects. J Clin Pharmacol. 1980;20:444–51.

41. May TW, Boor R, Mayer T, Jurgens U, Rambeck B, Holert N, *et al*. Concentrations of stiripentol in children and adults with epilepsy: the influence of dose, age, and comedication. Ther Drug Monit. 2012;34:390–7.

42. Tran A, Vauzelle-Kervroedan F, Rey E, Pous G, d'Athis P, Chiron C, *et al*. Effect of stiripentol on carbamazepine plasma concentration and metabolism in epileptic children. Eur J Clin Pharmacol. 1996;50: 497–500.

43. Perez J, Chiron C, Musial C, Rey E, Blehaut H, d'Athis P, *et al*. Stiripentol: efficacy and tolerability in children with epilepsy. Epilepsia. 1999;40:1618–26.

44. Maharaj AR, Barrett JS, Edginton AN. A workflow example of PBPK modeling to support pediatric research and development: case study with lorazepam. AAPS J. 2013;15:455–64.

45. Pullar T, Haigh JR, Peaker S, Feely MP. Pharmacokinetics of N-desmethylclobazam in healthy volunteers and patients with epilepsy. Br J Clin Pharmacol. 1987;24:793–7.

46. Vallner JJ, Needham TE, Jun HW, Brown WJ, Stewart JT, Kotzan JA, *et al*. Plasma levels of clobazam after three oral dosage forms in health subjects. J Clin Pharmacol. 1978;18:319–24.

47. Rupp W, Badian M, Christ O, Hajdu P, Kulkarni RD, Taeuber K, *et al*. Pharmacokinetics of single and multiple doses of clobazam in humans. Br J Clin Pharmacol. 1979;7 Suppl 1:51S–7S.

48. L. Inc. Onfi (clobazam) Tablets for oral use: prescribing information 2011.

49. Volz M, Christ O, Kellner HM, Kuch H, Fehlhaber HW, Gantz D, *et al*. Kinetics and metabolism of clobazam in animals and man. Br J Clin Pharmacol. 1979;7 Suppl 1:41S–50S.